Intersystem-Crossing Dynamics and Coordination Geometry Changes Observed by Ultrasonic and Laser Temperature-Jump Relaxation of the $^2T \rightleftharpoons {}^6A$ Spin Equilibrium of Hexadentate Iron(III) Complexes in Solution

Robert A. Binstead,*[1a] James K. Beattie,[1a] T. G. Dewey,[1b] and Douglas H. Turner[1b]

Contribution from the School of Chemistry, The University of Sydney, Sydney, N.S.W. 2006, Australia, and the Department of Chemistry, University of Rochester, Rochester, New York 14627. *Received February 29, 1980*

Abstract: Ultrasonic relaxation techniques have been employed to investigate the dynamics of the spin equilibrium of $[Fe(acac_2trien)]NO_3$ in aqueous solution and the coordination geometry changes associated with the iron(III) $\Delta S = 2$ intersystem-crossing process. For solutions of $[Fe(acac_2trien)]NO_3$ in an aqueous medium, single ultrasonic relaxations were observed. From the relaxation amplitudes the volume difference, $\Delta V°$, between the high-spin and low-spin states is calculated to be 10.3 ± 0.2 cm^3 mol^{-1}. This volume difference corresponds to an estimated difference in average metal–ligand bond lengths of 0.11 Å. For $[Fe(Sal_2trien)]NO_3 \cdot H_2O$ in aqueous solution, the difference in average metal–ligand bond lengths is estimated to be 0.13 Å. These estimates are in excellent agreement with the X-ray structural data for these complexes. The ultrasonic relaxation time for the interconversion between the low-spin doublet and high-spin sextet states of $[Fe(acac_2trien)]^+$ is 2.11 ± 0.04 ns at 25 °C in aqueous solution. This value is consistent with the spectroscopic observation of a relaxation time less than the ~13-ns heating rise time of the Raman laser temperature-jump apparatus. From the relaxation time and the equilibrium constant, K_{26}, of 0.491, measured by using the Evans ^{1}H NMR technique, the forward (k_{26}) and reverse (k_{62}) rate constants at 25 °C have been calculated to be 1.56×10^8 s^{-1} and 3.18×10^8 s^{-1}, respectively. The temperature dependence of the rate constants implies activation enthalpies of $\Delta H_{26}^{\ddagger} = 6.38 \pm 0.17$ kcal mol^{-1} and $\Delta H_{62}^{\ddagger} = 2.40 \pm 0.17$ kcal mol^{-1}. With use of the absolute rate theory, the minimum value of the transmission coefficient κ is calculated to be $10^{-2.5}$ for this formally spin-forbidden $\Delta S = 2$ intersystem-crossing process. The rate constants for intersystem crossing are thus determined by both electronic factors and the thermodynamic barriers associated with the structural reorganization. This process can therefore be described as a nonadiabatic, internal electron transfer between two distinct electronic isomers possessing different nuclear configurations.

Introduction

The thermal spin state equilibria of first-row transition-metal complexes are examples of nonradiative, spin-forbidden electronic transitions, generally referred to as intersystem-crossing processes. Since these spin equilibria are ground-state processes, they provide a convenient means of investigating the dynamics of intersystem-crossing processes which are otherwise only accessible in excited states, where other competitive deactivation pathways may also occur.[2] Therefore, the assessment of the factors which determine the rates of spin state interconversions is important for understanding the role of intersystem crossing in the photochemistry and photophysics of the excited states of transition-metal complexes. Furthermore, their kinetics are important for determining the effect of spin-multiplicity changes on the rates of bimolecular electron-transfer reactions.

Using ultrasonic relaxation techniques, we have previously measured the rates of intersystem crossing between the singlet and quintet states of $[Fe(HB(pz)_3)_2]$ in THF and of $[Fe(paptH)_2]Cl_2 \cdot 2H_2O$ in H_2O[3] and between the doublet and sextet states of $[Fe(Sal_2trien)]NO_3 \cdot H_2O$ in H_2O.[4] In each case single ultrasonic relaxations were observed with concentration-independent relaxation times, as expected for unimolecular isomerizations between spin states. For $[Fe(HB(pz)_3)_2]$ in THF a relaxation time of 33.0 ± 0.7 ns was observed at 25 °C in agreement with the value of 32 ± 10 ns observed spectrophotometrically for CH_2Cl_2–MeOH solutions at 25 °C using the Raman laser temperature-jump technique.[5] For $[Fe(Sal_2trien)]NO_3 \cdot H_2O$ (compound I) in H_2O a relaxation time of 8.94 ± 0.16 ns was observed

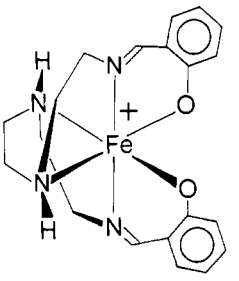

I

at 5 °C compared with a value of 38 ± 4 ns at 4 °C reported by Wilson et al. using the Raman laser temperature-jump technique.[6] Since the laser temperature-jump experiments were performed at a lower concentration than the ultrasonic relaxation experiments, it has been suggested by Wilson et al. that there may be a concentration dependence of the relaxation time.[6] However, no such concentration dependence was observed in the ultrasonic relaxation experiments over the twofold concentration range experimentally accessible. To test further for a possible concentration dependence of the relaxation times, we now report observations of ultrasonic relaxations ascribed to the spin equilibrium (eq 1) of $[Fe(acac_2trien)]NO_3$ (compound II) in aqueous solution over a fivefold concentration range, together with independent observations of the spin state relaxations of $[Fe(Sal_2trien)]NO_3 \cdot H_2O$ and [Fe-

$$^2T \underset{k_{62}}{\overset{k_{26}}{\rightleftharpoons}} {}^6A \qquad (1)$$

(1) (a) University of Sydney. (b) University of Rochester.
(2) (a) Martin, R. L.; White, A. H. *Transition Met. Chem.* **1968**, *4*, 113. (b) Kasha, M. *Discuss. Faraday Soc.* **1950**, *9*, 14. (c) Balzani, V.; Carassiti, V. "Photochemistry of Coordination Compounds"; Academic Press: New York, 1970.
(3) Beattie, J. K.; Binstead, R. A.; West, R. J. *J. Am. Chem. Soc.* **1978**, *100*, 3044.
(4) Binstead, R. A.; Beattie, J. K.; Dose, E. V.; Tweedle, M. F.; Wilson, L. J. *J. Am. Chem. Soc.* **1978**, *100*, 5609.
(5) Beattie, J. K.; Sutin, N.; Turner, D. H.; Flynn, G. W. *J. Am. Chem. Soc.* **1973**, *95*, 2052.
(6) Dose, E. V.; Hoselton, M. A.; Sutin, N.; Tweedle, M. F.; Wilson, L. J. *J. Am. Chem. Soc.* **1978**, *100*, 1141.

0002-7863/80/1502-6442$01.00/0

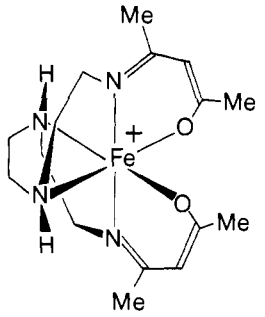

II

(acac$_2$trien)]NO$_3$ in both aqueous and methanol solutions using the Raman laser temperature-jump technique.

The volume differences, $\Delta V°$, between the high-spin and low-spin states of both [Fe(Sal$_2$trien)]$^+$ and [Fe(acac$_2$trien)]$^+$ have been determined both from the ultrasonic relaxation amplitudes and from independent measurements of the pressure dependence of the equilibrium constants. Furthermore, the values of $\Delta V°$ obtained from the relaxation amplitudes have been used to evaluate the coordination geometry changes accompanying these spin state isomerizations. Finally, from the temperature dependence of the relaxation times we have assessed the barriers to these intersystem-crossing processes and have calculated lower limits for the probability of the spin-forbidden intersystem crossing in these pseudooctahedral d^5 complexes.

Experimental Section

Materials. Acetylacetone (Merck AR), triethylenetetramine (Eastman Kodak, technical grade), sodium methoxide (Fluka, practical grade), and ferric nitrate nonahydrate (Merck AR) were used without further purification to prepare the complex [Fe(acac$_2$trien)]NO$_3$.

The ligand, acac$_2$trien, was prepared by adding a solution of triethylenetetramine (5.85 g, 40 mmol) in 15 mL of MeOH (Merck AR) dropwise via Pasteur pipette to a stirred solution of acetylacetone (10.00 g, 100 mmol) in 20 mL of MeOH, resulting in a yellow solution, which was stirred for 30 min. To this stirred solution was added slowly via Pasteur pipette a solution of NaOCH$_3$ (5.40 g, 100 mmol) in 90 mL of MeOH, the resulting ligand solution being stirred for a further 15 min.

The complex [Fe(acac$_2$trien)]NO$_3$ was prepared by adding a solution of Fe(NO$_3$)$_3$·9H$_2$O (16.16 g, 40 mmol) in 50 mL of MeOH dropwise via Pasteur pipette to the stirred ligand solution. The resulting deep red-purple solution was stirred for a further 30 min, filtered, and taken to dryness by rotary evaporation. The crude solid was extracted with 8 × 200 mL volumes of CH$_2$Cl$_2$ (Merck AR) until only a dark brown solid remained. This brown impurity was removed by filtration from each extract. The combined filtrates were reduced in volume to ~300 mL by rotary evaporation. The addition of ~100 mL of CCl$_4$ (Merck AR) and further removal of CH$_2$Cl$_2$ precipitated a black-purple product which was collected by filtration, washed with CCl$_4$ until the washings were colorless, then washed with 100-mL volumes of diethyl ether (Merck UVASOL), acetone (Merck AR), and diethyl ether again, and air dried. This black-purple product was purified by recrystallizing it twice from CH$_2$Cl$_2$–CCl$_4$ as above and drying in vacuo over P$_4$O$_{10}$ for 24 h at 90 °C, yielding 7.35 g (43%) of black-purple microcrystalline complex. Anal. Calcd for C$_{16}$H$_{28}$N$_5$O$_5$Fe: C, 45.08; H, 6.62; N, 16.43; O, 18.77; Fe, 13.10. Found: C, 44.91; H, 6.58; N, 16.51; O, 18.93; Fe, 13.00.

As previously noted, the complex slowly hydrolyzes in aqueous solution producing some Fe(OH)$_3$ precipitate. However, the rate of hydrolysis was observed to be pH dependent, with rate constants k(pH 10) ≪ k(pH 7) ≪ k(pH 4). Consequently, measurements in aqueous media were obtained at pH 10, as far as practicable. Merck pH 10 buffer solution was used as the solvent for the magnetic susceptibility and ultrasonic relaxation measurements.[17] The variable-temperature electronic spectral measurements and laser temperature-jump kinetic measurements were obtained in aqueous 10^{-4} M KOH solutions. However, the short time scales for the density measurements (20 minutes) and variable pressure electronic absorption measurements allowed the use of unbuffered, distilled water as the solvent. This eliminated the necessity for uncertain buffer corrections to these data.

The complex [Fe(Sal$_2$trien)]NO$_3$·H$_2$O was prepared as described previously,[7] purified by recrystallizing it twice from distilled water, and dried in vacuo at room temperature for 24 h over P$_4$O$_{10}$. Anal. Calcd for C$_{20}$H$_{26}$N$_5$O$_6$Fe: C, 49.19; H, 5.37; N, 14.34; O, 19.66; Fe, 11.44. Found: C, 49.16; H, 5.31; N, 14.50; O, 19.51; Fe, 11.50. As this complex is very stable in aqueous solution, no buffer was required. Hence, all the physical measurements for aqueous solutions of the complex were obtained by using distilled water as the solvent.

Methods. Magnetic susceptibility measurements for a 0.05 M solution of [Fe(acac$_2$trien)]NO$_3$ in pH 10 buffer and for 0.02 M solutions of [Fe(Sal$_2$trien)]NO$_3$·H$_2$O in both distilled water and methanol were obtained by using the Evans ^{1}H NMR technique[8] (see below) at 90 MHz (Bruker HX-90 with Quadrature Detection). An internal reference of 4% v/v t-BuOH was used for aqueous solutions. For methanol solutions the solvent methyl peak was used for shift measurements. The sample temperatures were measured with internal capillaries of ethylene glycol (Merck AR)[9] and methanol (Merck AR)[10] for aqueous and methanol solutions, respectively. The validity of these literature temperature calibrations was checked against the melting points of several pure organic liquids and solids.

The measured shift values, Δf (Hz), obtained by using the Evans technique are related to the mass susceptibility of the solute, χ_g, by eq 2, where χ_0 is the mass susceptibility of the solvent, m_0 is the mass of

$$\chi_g = \frac{3}{2\pi}\frac{\Delta f}{f m_0} + \chi_0 + \chi_0\frac{(d_0 - d_s)}{m_0} \quad (2)$$

solute per cubic centimeter, d_s and d_0 are the densities of the solution and solvent (g cm^{-3}), respectively, and f is the spectrometer frequency (Hz).[8] Crawford and Swanson have presented in the literature a method for the calculation of magnetic moments using the Evans equation (2).[11] However, these authors have incorrectly indicated χ_0 as positive in sign in their sample calculations. This confusion caused slight miscalculations of the magnetic moments in previous work.[3,4] Rather, the sign of χ_0 is negative and hence the third term of the Evans equation makes a positive contribution to χ_g in *most* solvents.[12] The third term of eq 2 is small and is usually neglected. However, this simplification can lead to large errors when the paramagnetic susceptibility is small, so that the third term should be evaluated wherever possible. The m_0 data were corrected for changes in solvent density and hence sample concentration with temperature.[13,14] Since the density difference $(d_0 - d_s)$ depends linearly on concentration, evaluation of these data was simplified by measuring the density difference at one temperature (25 °C) and correcting for the changes in sample concentration with temperature, leading to eq 3, which simplifies to eq 4, where m_0^{25} is the mass of solute per cubic centimeter at 25 °C and $d_0^{25} - d_s^{25}$ is the density difference (g cm^{-3}) at 25 °C. The third term of the Evans equation can therefore be seen to be independent of temperature.

$$\chi_g = \frac{3}{2\pi}\frac{\Delta f}{f m_0} + \chi_0 + \frac{\chi_0}{m_0}(d_0^{25} - d_s^{25})\frac{m_0}{m_0^{25}} \quad (3)$$

$$\chi_g = \frac{3}{2\pi}\frac{\Delta f}{f m_0} + \chi_0 + \frac{\chi_0(d_0^{25} - d_s^{25})}{m_0^{25}} \quad (4)$$

The molar susceptibility, χ_M^{cor}, was obtained by multiplying χ_g by the molecular weight (M_r) and correcting for ligand and anion diamagnetism, χ_D, using eq 5, where the sign of χ_D is negative. The magnetic moments were then calculated by using eq 6. The estimated maximum error in the magnetic moment is ±0.1 μ_B but the probable error is estimated to be ±0.03 μ_B.

$$\chi_M^{cor} = (\chi_g \times M_r) - \chi_D \quad (5)$$

$$\mu_{eff} = 2.828(\chi_M^{cor} T)^{1/2} \quad (6)$$

Density difference measurements were obtained at 25.0 °C by using an Anton Paar (Graz, Austria) DMA-02C precision density meter. The sample temperature was controlled by circulating water from a precision-temperature bath through the thermostating block of the density meter. The temperature fluctuations in the bath were controlled to

(7) Tweedle, M. F.; Wilson, L. J. *J. Am. Chem. Soc.* **1976**, *98*, 4824.
(8) Evans, D. F. *J. Chem. Soc.* **1959**, 2003.
(9) Kaplan, M. L.; Bovey, F. A.; Cheng, H. N. *Anal. Chem.* **1975**, *47*, 1703.
(10) van Geet, A. L. *Anal. Chem.* **1970**, *42*, 679.
(11) Crawford, T. H.; Swanson, J. *J. Chem. Educ.* **1971**, *48*, 382.
(12) Joedicke, I. B.; Studer, H. V.; Yoke, J. T. *Inorg. Chem.* **1976**, *15*, 1352.
(13) Weast, R. C., Ed. "Handbook of Chemistry and Physics", 56th ed.; CRC Press: Cleveland, 1976.
(14) Riddick, J. A.; Bunger, W. "Techniques of Chemistry", 3rd ed.; Weissberger, A. Ed.; Wiley-Interscience: New York, 1970; Vol. II.

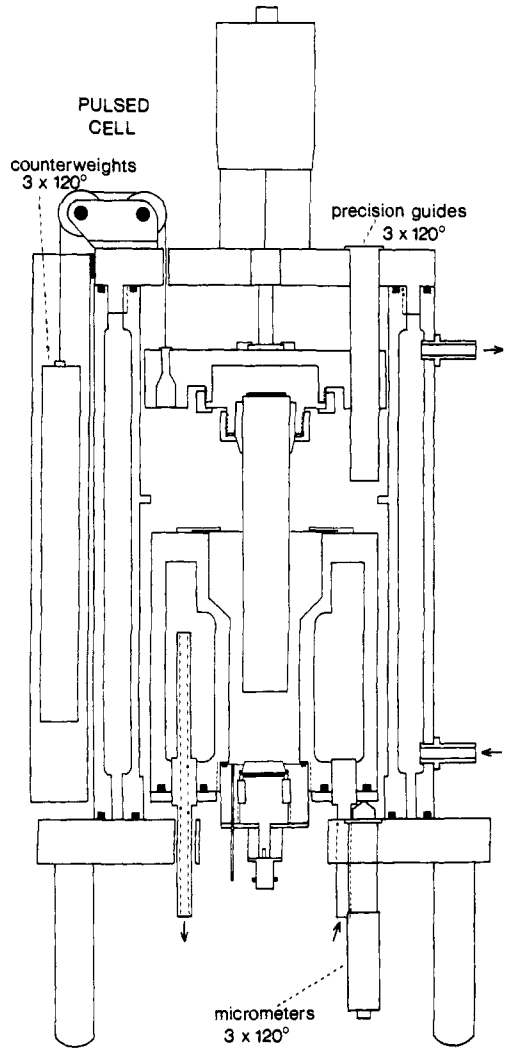

Figure 1. Cross-sectional diagram of the pulsed ultrasonic cell.

±0.0005 °C by using a Bayley Instruments Co. (Danville, Calif.) Model 121 precision temperature controller. With the room temperature controlled to 25 ± 0.5 °C by air conditioning, density difference measurements were obtained precise to $\pm 3 \times 10^{-6}$ g cm^{-3} for aqueous solutions and to $\pm 3 \times 10^{-5}$ g cm^{-3} for methanol solutions.

Variable-temperature electronic spectral measurements were obtained by using a Varian Techtron 635 spectrophotometer and jacketed quartz cells in conjunction with a Colora WK-5 refrigerated constant-temperature bath. The data were corrected for changes in solvent density and hence sample concentration with temperature.[13,14]

Variable-pressure electronic spectral measurements were obtained at the University of Melbourne by using a Varian Techtron 635D spectrophotometer fitted with a thermostated high-pressure cell in the sample beam.[15] The temperature reequilibrium time of the sample after the application or release of pressure was about 3 min. Single wavelength absorbance measurements were recorded at 25 °C, over the pressure range 1–1367 atm. The data were corrected for changes in solvent density and hence sample concentration with pressure.[16]

Ultrasonic absorption measurements were made in the range 10–200 MHz by using the pulsed ultrasonic cell shown in Figure 1, whose operation has been described previously[3] and is illustrated schematically in Figure 2. The performance of this apparatus has been improved for this work by the addition of high-precision Kay Elemetrics (Pine Brook, N.J.) 500A 1.0 dB/step and 1/500A 0.1 dB/step rotary references attenuators. Matec Inc. (Warwick, R.I.) Models 70 and 80 impedance matching networks have been substituted for our earlier devices to improve both the signal amplitude from the ultrasonic cell and to provide exactly 50 Ω impedance loads to the Wide Band Engineering (Phoenix, Ariz.) A73 directional coupler and A66-GA precision hybrid combiner, resulting in maximum isolation between the reference and signal lines. For frequencies above 50 MHz the signal to noise ratio has been improved by substituting Wide Band Engineering A52 and A82-H R.F. amplifiers and a custom made R.F. detector in place of the earlier VHF receiver.[27]

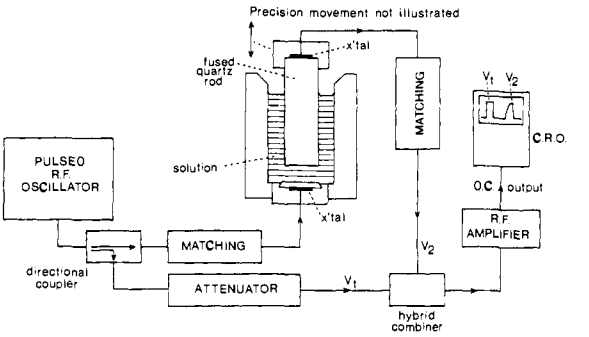

Figure 2. Schematic diagram of the pulsed ultrasonic absorption technique.

The ultrasonic absorption measurements for [Fe(acac$_2$trien)]NO$_3$ were made in Merck pH 10 buffer solution.[17] The ultrasonic absorption of this buffer is indistinguishable from pure water, and there is no evidence of any relaxational excess absorption in the frequency range 10–200 MHz. The solutions of the complex were filtered through a 1.0 μm Millipore filter prior to use to remove a faint trace of Fe(OH)$_3$ which could not be removed by repeated recrystallization. Sample decomposition over the timescale of the ultrasonic experiment was checked by refiltering the solution through a 1.0 μm Millipore after ~6 h. At the highest temperature studied, 25 °C, only a tiny amount of Fe(OH)$_3$ was removed, indicating negligible decomposition. At 5 °C there was no detectable decomposition at all.

Temperature-jump experiments were performed at the University of Rochester by using a Raman laser temperature-jump apparatus which has been described previously.[18] Measurements were made by using cells with path lengths of either 0.1 or 1 mm. The solutions were thermostated by circulating a water–ethylene glycol mixture from a refrigerated constant-temperature bath (Haake FS2 and C-50) through a metal block to which the cells were attached. The initial temperatures of the solutions were measured with a thermocouple attached to the thermostating block. The cross-sectional area of solution actually heated by the 1.41-μm 1-J, laser pulse was estimated from burn patterns to be ~0.5 cm^2, resulting in calculated temperature jumps of 2.8 °C for methanol solutions and 4.3 °C for aqueous solutions in 1-mm path length cells. The apparent relaxation times were estimated either directly from photographs of the oscilloscope traces or from plots of ln $(I_\infty - I)$ vs. time.

Results

The ultrasonic absorption of 0.020 and 0.100 M solutions of [Fe(acac$_2$trien)]NO$_3$ in pH 10 buffer (Figure 3) are described by single relaxation curves according to eq 7, where α is the

$$\alpha/f^2 = A(1 + \omega^2\tau^2)^{-1} + B \qquad (7)$$

absorption coefficient (Np cm^{-1}), f is the frequency (Hz), ω is the angular frequency (rad s^{-1}) = $2\pi f$, τ is the relaxation time (s), A is the amplitude, and B is the background absorption for a particular relaxation curve. The least-squares fitted values of A, B, and τ are listed in Table I; the relaxation time was found to be concentration independent.

To interpret these results, it is necessary to know the equilibrium constants and thermodynamic parameters associated with the spin equilibrium (eq 1) under the conditions of the ultrasonic measurements. Therefore, solution magnetic susceptibility measurements were used to characterize the spin equilibrium of [Fe(acac$_2$trien)]NO$_3$ in an aqueous pH 10 buffer solution at 0.05 M between 1.1 and 53.7 °C, and these data are listed in Table II (supplementary material). The equilibrium constants were calculated from the expression $K_{26} = (\mu_{eff}^2 - \mu_{LS}^2)/(\mu_{HS}^2 - \mu_{eff}^2)$, where μ_{HS} and μ_{LS} are the limiting high-spin and low-spin magnetic moments, respectively. The value of μ_{HS} was fixed at 5.92 μ_B, the spin-only value for the ^{6}A state. The value of μ_{LS} was taken

(15) Lawrance, G. A.; Stranks, D. R. *Inorg. Chem.* **1978**, *17*, 1804.
(16) Grindley, T.; Lind J. E., Jr. *J. Chem. Phys.* **1971**, *54*, 3983.
(17) Merck pH 10 buffer solution consists of a mixture of KOH, KCl, and boric acid.
(18) (a) Dewey, T. G.; Turner, D. H. *Adv. Mol. Relaxation Interact. Processes* **1978**, *13*, 331. (b) Turner, D. H.; Flynn, G. W.; Sutin, N.; Beitz, J. V. *J. Am. Chem. Soc.* **1972**, *94*, 1554.

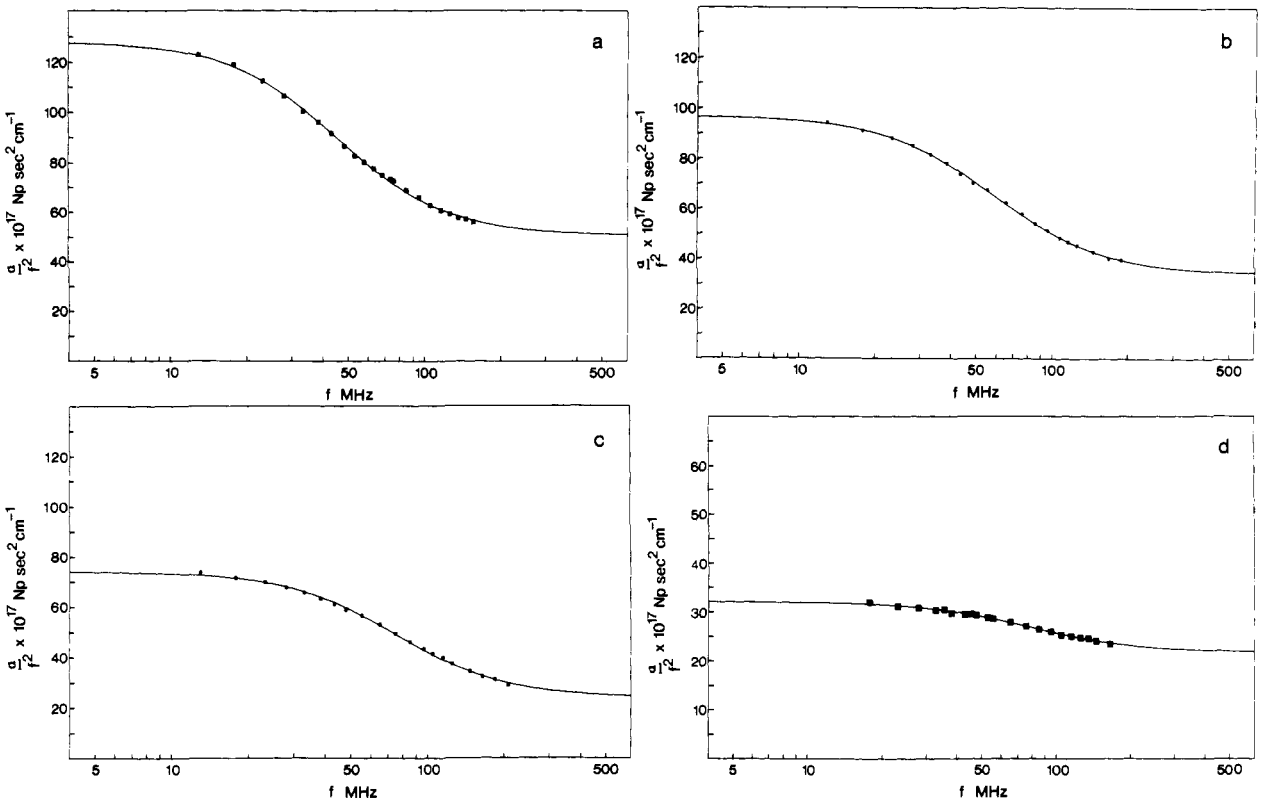

Figure 3. Ultrasonic absorption curves for [Fe(acac$_2$trien)]NO$_3$ in pH 10 buffer: (a) 0.100 M, 5 °C; (b) 0.100 M, 15 °C; (c) 0.100 M, 25 °C; (d) 0.020 M, 25 °C.

Table I. Collected Data and Results for [Fe(acac$_2$trien)]NO$_3$ in pH 10 Buffer[a]

	5 °C	15 °C	25 °C
$10^{17}A$, Np s^2 cm^{-1}	77.4 ± 0.8	62.9 ± 0.5	50.2 ± 0.6
$10^{17}B$, Np s^2 cm^{-1}	50.4 ± 0.5	34.0 ± 0.3	23.9 ± 0.5
τ, ns	3.46 ± 0.06	2.72 ± 0.03	2.11 ± 0.04
μ_{eff},[b] μ_B	3.35	3.56	3.77
K_{26}	0.303	0.389	0.491
$\Delta H°$, kcal mol^{-1}			3.98 ± 0.02
$\Delta S°$, cal deg^{-1} mol^{-1}			11.93 ± 0.07
C_{total}, M	0.1002	0.1000	0.1000[d]
$10^5\Gamma$, mol cm^{-3}	1.79	2.02	2.21
ρ,[c] g cm^{-3}	0.99999	0.99913	0.99707
v,[c] cm s^{-1}	144900	147300	149700
$\alpha_P/\rho C_p$,[c] cm^3 kcal^{-1}	0.01592	0.15090	0.25825
$\Delta V°$, cm^3 mol^{-1}	10.12	10.32	10.55
k_{26}, s^{-1}	6.72×10^7	1.03×10^8	1.56×10^8 [e]
k_{62}, s^{-1}	2.22×10^8	2.65×10^8	3.18×10^8 [e]
$\Delta G_{26}^{\ddagger}$, kcal mol^{-1}			6.28 ± 0.03[f]
$\Delta G_{62}^{\ddagger}$, kcal mol^{-1}			5.85 ± 0.02[f]
$\Delta H_{26}^{\ddagger}$, kcal mol^{-1}			6.38 ± 0.17
$\Delta H_{62}^{\ddagger}$, kcal mol^{-1}			2.40 ± 0.17
$\Delta S_{26}^{\ddagger}$, cal deg^{-1} mol^{-1}			0.34 ± 0.61
$\Delta S_{62}^{\ddagger}$, cal deg^{-1} mol^{-1}			−11.59 ± 0.60

[a] The quoted error bars are for one standard deviation. [b] The estimated error is ±0.03 μ_B. [c] Pure solvent values were assumed for the physical constants. [d] At 0.02005 M, $A = (10.3 \pm 0.3) \times 10^{-17}$ Np s^2 cm^{-1}, $B = (21.7 \pm 0.2) \times 10^{-17}$ Np s^2 cm^{-1}, and $\tau = (2.04 \pm 0.09)$ ns. [e] The standard deviations for k_{26} and k_{62} at 25 °C are calculated to be ±4.1% and ±3.0%, respectively, on the basis of the quoted uncertainties in τ and μ_{eff}. [f] The free energies of activation and estimated errors were calculated directly from the rate constants and their uncertainties by using eq 15.

as 2.0 μ_B, as found previously.[19] With these limiting moments the data give a straight line plot of log K_{26} vs. T^{-1} (Figure 4) with a $\Delta H°$ of 3.98 ± 0.02 kcal mol^{-1} and $\Delta S°$ of 11.93 ± 0.07 cal deg^{-1} mol^{-1}.

(19) Dose, E. V.; Murphy, K. M. M.; Wilson, L. J. *Inorg. Chem.* **1976**, *15*, 2622.

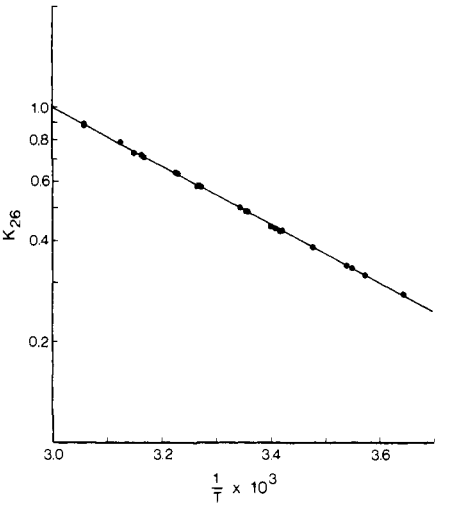

Figure 4. Temperature dependence of the equilibrium constant K_{26} for [Fe(acac$_2$trien)]NO$_3$ in pH 10 buffer.

Solution magnetic susceptibility measurements were also made for a 0.02 M solution of [Fe(Sal$_2$trien)]NO$_3$·H$_2$O in H$_2$O over the range 4.9–77.7 °C in order to improve the precision of the results obtained previously,[4] and these data are listed in Table III (supplementary material). The higher precision of the present data, obtained over a wider temperature range, clearly reveals that the value of μ_{LS} in aqueous solution cannot be 1.9 μ_B. A value of 3.0 μ_B is required for μ_{LS} to obtain a linear plot of log K_{26} vs. T^{-1} (Figure 5). With limiting moments of 5.92 and 3.0 μ_B, the data were fitted by linear least-squares regression yielding a $\Delta H°$ of 5.11 ± 0.03 kcal mol^{-1} and a $\Delta S°$ of 15.70 ± 0.08 cal deg^{-1} mol^{-1}.

The value of 3.0 μ_B for μ_{LS} is somewhat surprising since previous measurements for the PF_6^- salt of this complex in a variety of organic solvents have indicated a value of 1.9 μ_B for μ_{LS}, close to the spin-only value due to effective quenching of the orbital angular momentum of the ^2T state.[7] Indeed, single-crystal X-ray

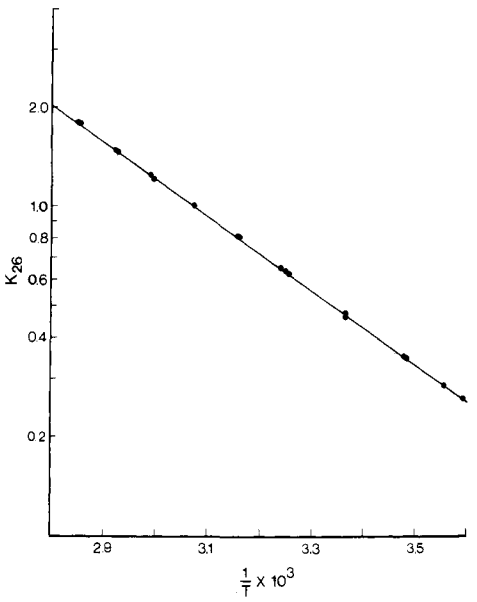

Figure 5. Temperature dependence of the equilibrium constant K_{26} for $[Fe(Sal_2trien)]NO_3 \cdot H_2O$ in distilled water.

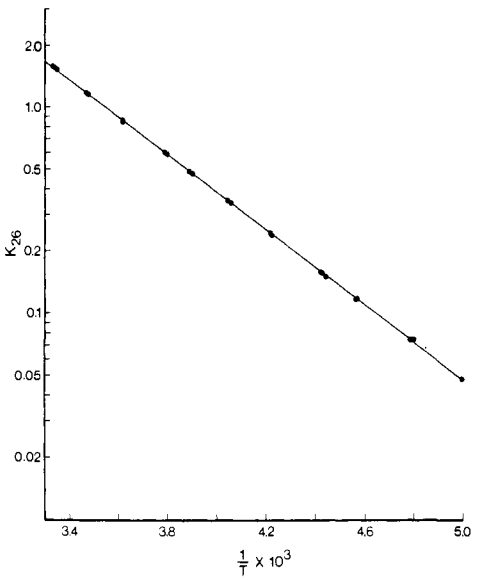

Figure 6. Temperature dependence of the equilibrium constant K_{26} for $[Fe(Sal_2trien)]NO_3 \cdot H_2O$ in methanol.

structural data have shown that the complex has a tetragonal distortion which would be expected to split the ^2T state into ^2A and ^2E states and hence quench the orbital angular momentum.[20] While the value of 3.0 μ_B for μ_{LS} is the value expected for a ^2T state with a full orbital angular momentum contribution, this seems unlikely in view of the tetragonal distortion in the complex. A more realistic explanation is the mixing in of the low-lying ^4E excited state via spin–orbit coupling since ligand field calculations have shown that for values of $10Dq$ near the crossover region, tetragonal axial distortions of only 1000 cm^{-1} can result in close proximity of the quartet and doublet states.[21] It would appear that the axial distortion varies with the nature of the solvent–solute interaction.

An alternative explanation for the high value of μ_{LS} could be a significant amount of high-spin impurity in the sample. This is unlikely in view of the excellent analytical results for all elements present. However, to eliminate this possibility, we also made magnetic susceptibility measurements in methanol solution for the same sample, and these data are listed in Table IV (supplementary material). With use of limiting moments of 5.92 and 1.90 μ_B a plot of log K_{26} vs. T^{-1} is perfectly linear over a 100 °C temperature range, as shown in Figure 6, in good agreement with the value of 1.90 μ_B previously found for μ_{LS}.[8] These data give a $\Delta H°$ of 4.16 ± 0.01 kcal mol^{-1} and a $\Delta S°$ of 14.73 ± 0.05 cal deg^{-1} mol^{-1}. Since the magnetic susceptibility data for $[Fe(Sal_2trien)]NO_3 \cdot H_2O$ in methanol solution fit so well to a limiting moment of 1.90 μ_B for μ_{LS}, there is certainly no significant amount of high-spin impurity in the sample. It should be noted, however, that the magnetic moment in solution is slightly anion dependent,[7] so that small differences in thermodynamic parameters may arise with different anions.

A measure of the volume difference, $\Delta V°$, between the low-spin and high-spin isomers of both $[Fe(acac_2trien)]^+$ and $[Fe(Sal_2trien)]^+$ can be obtained from the amplitudes of their ultrasonic relaxations. Equation 7 can be rewritten as eq 8. Hence,

$$\frac{\alpha}{f^2} = \frac{2\pi^2\rho v}{RT}\left(\Delta V° - \frac{\alpha_P}{\rho C_P}\Delta H°\right)^2 \frac{\Gamma\tau}{1+\omega^2\tau^2} + B \qquad (8)$$

the excess ultrasonic absorption for $\omega \ll \tau^{-1}$ is given in eq 9, where

$$A = \frac{2\pi^2\rho v}{RT}\left(\Delta V° - \frac{\alpha_P}{\rho C_P}\Delta H°\right)^2 \Gamma\tau \qquad (9)$$

Table V. Collected Data and Results for $[Fe(Sal_2trien)]NO_3 \cdot H_2O$ in H_2O[a]

	5 °C	15 °C	25 °C
$10^{17}A$, Np s^2 cm^{-1}	38.0 ± 0.4	52.3 ± 0.3	39.9 ± 0.2
$10^{17}B$, Np s^2 cm^{-1}	45.2 ± 0.3	29.9 ± 0.2	21.4 ± 0.2
τ, ns	8.94 ± 0.16	6.80 ± 0.06	5.33 ± 0.05
μ_{eff},[b] μ_B	3.79	3.99	4.19
K_{26}	0.262	0.361	0.486
$\Delta H°$, kcal mol^{-1}			5.11 ± 0.03
$\Delta S°$, cal deg^{-1} mol^{-1}			15.70 ± 0.08
C_{total}, M	0.01504	0.02579	0.02546[d]
$10^6\Gamma$, mol cm^{-3}	2.47	5.02	5.61
ρ,[c] g cm^{-3}	0.99999	0.99913	0.99707
v,[c] cm s^{-1}	144900	147300	149700
$\alpha_P/\rho C_p$,[c] cm^3 kcal^{-1}	0.01592	0.15090	0.25825
$\Delta V°$, cm^3 mol^{-1}	11.87	12.01	11.92
k_{26}, s^{-1}	2.32×10^7	3.90×10^7	6.14×10^7 [e]
k_{62}, s^{-1}	8.87×10^7	1.08×10^8	1.26×10^8 [e]
$\Delta G_{26}^{\ddagger}$, kcal mol^{-1}			6.83 ± 0.02[f]
$\Delta G_{62}^{\ddagger}$, kcal mol^{-1}			6.40 ± 0.01[f]
$\Delta H_{26}^{\ddagger}$, kcal mol^{-1}			7.45 ± 0.29
$\Delta H_{62}^{\ddagger}$, kcal mol^{-1}			2.34 ± 0.29
$\Delta S_{26}^{\ddagger}$, cal deg^{-1} mol^{-1}			2.1 ± 1.0
$\Delta S_{62}^{\ddagger}$, cal deg^{-1} mol^{-1}			−13.6 ± 1.0

[a] The quoted error bars are for one standard deviation. [b] The estimated error is ±0.03 μ_B. [c] Pure solvent values were assumed for the physical constants. [d] At 0.01297 M, $A = (20.2 \pm 0.3) \times 10^{-17}$ Np s^2 cm^{-1}, $B = (20.9 \pm 0.3) \times 10^{-17}$ Np s^2 cm^{-1}, and $\tau = (5.16 \pm 0.15)$ ns. [e] The standard deviations for k_{26} and k_{62} at 25 °C are calculated to be ±3.9% and ±2.4%, respectively, on the basis of the quoted uncertainties in τ and μ_{eff}. [f] The free energies of activation and their estimated errors were calculated directly from the rate constants and their uncertainties by using eq 15.

ρ is the solution density (g cm^{-3}), v the sound velocity (cm s^{-1}), α_P the coefficient of thermal expansion (deg^{-1}), C_P the specific heat (cal deg^{-1} g^{-1}) and Γ the concentration dependence (mol cm^{-3}) $\{\Gamma^{-1} = 1000([LS]^{-1} + [HS]^{-1})$ where [LS] and [HS] are the molar concentrations of the low-spin and high-spin isomers, respectively$\}$.[22] Values of $\Delta H°$ and Γ were obtained from the determination of the equilibrium constants by the NMR method. The values of the physical constants were assumed to be those for pure water.[13,14]

For $[Fe(acac_2trien)]^+$ in aqueous solution the values of the physical constants and relaxation parameters obtained in this work

(20) Sinn, E.; Sim, G.; Dose, E. V.; Tweedle, M. F.; Wilson, L. J. *J. Am. Chem. Soc.* **1978**, *100*, 3375.
(21) Konig, E.; Kremer, S. "Ligand Field Energy Diagrams"; Plenum Press: New York, 1977.
(22) Steuhr, J. "Techniques of Chemistry", 3rd ed.; Weissberger, A., Ed.; Wiley-Interscience: New York, 1974; Vol. VI, Part II, p 237.

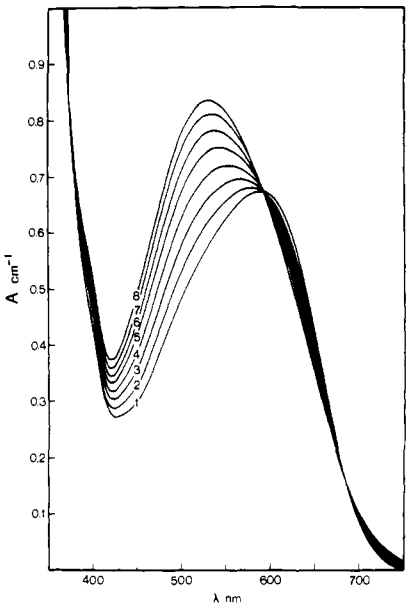

Figure 7. Temperature dependence of the electronic absorption spectrum of a 5 × 10^{-4} M solution of [Fe(acac$_2$trien)]NO$_3$ in distilled water at pH 10: (1) 5 °C, (2) 15 °C, (3) 25 °C, (4) 35 °C, (5) 45 °C, (6) 55 °C, (7) 65 °C, (8) 75 °C.

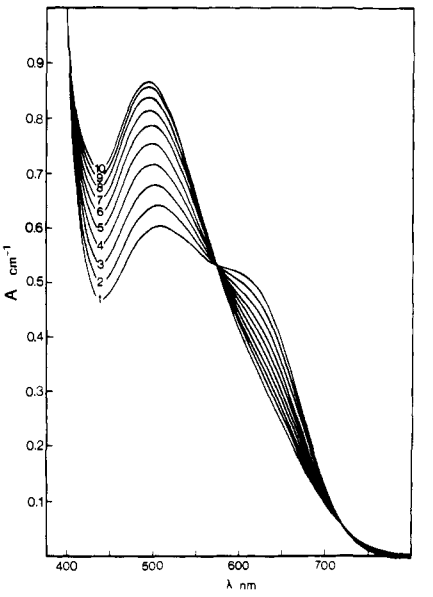

Figure 8. Temperature dependence of the electronic absorption spectrum of a 3 × 10^{-4} M solution of [Fe(Sal$_2$trien)]NO$_3$·H$_2$O in distilled water: (1) 5 °C, (2) 15 °C, (3) 25 °C, (4) 35 °C, (5) 45 °C, (6) 55 °C, (7) 65 °C, (8) 75 °C, (9) 85 °C, (10) 95 °C.

are listed in Table I, while those obtained previously for [Fe(Sal$_2$trien)]$^+$ in distilled water are listed in Table V, together with the values of $\Delta V°$ calculated at three different temperatures in each case. Values of 10.3 ± 0.2 and 11.9 ± 0.1 cm^3 mol^{-1} were obtained for the volume differences between the doublet and sextet states of [Fe(acac$_2$trien)]$^+$ and [Fe(Sal$_2$trien)]$^+$, respectively. Since these two complexes have about the same molecular weight, and hence molar volume, the similarity of their $\Delta V°$ values indicates that the metal–ligand bond length differences between their respective low-spin and high-spin states are nearly the same. Furthermore, even though the ultrasonic relaxation amplitudes vary with temperature, the $\Delta V°$ values are constant, showing that the relaxation amplitudes are consistent with the temperature dependences of the spin equilibria.

It is possible to verify independently the values of $\Delta V°$ obtained from the relaxation amplitudes by determining the pressure dependence of the equilibrium constants. Since the electronic absorption spectra of both [Fe(acac$_2$trien)]$^+$ and [Fe(Sal$_2$trien)]$^+$ are the superposition of bands due to the doublet and sextet isomers, changes in their equilibrium constants with temperature or pressure are reflected in their spectra. The temperature dependences of the electronic absorption spectra of [Fe(acac$_2$trien)]$^+$ and [Fe(Sal$_2$trien)]$^+$ in aqueous solutions are shown in Figures 7 and 8, respectively. These spectra reveal clean isosbestic points in both cases, as expected for unimolecular isomerizations between two different electronic species. At a single wavelength λ, therefore, the absorbance for a 1-cm path length, A_λ, is given by eq 10, where ϵ_{obsd} is the observed molar absorptivity and ϵ_{LS} and

$$A_\lambda = \epsilon_{obsd}([LS] + [HS]) = \epsilon_{LS}[LS] + \epsilon_{HS}[HS] \quad (10)$$

ϵ_{HS} are the molar absorptivities of the low-spin and high-spin isomers, respectively. Since $K_{26} = [HS]/[LS]$, then

$$(K_{26} + 1)\epsilon_{obsd} = \epsilon_{LS} + K_{26}\epsilon_{HS} \quad (11)$$

Therefore, a plot of $(K_{26} + 1)\epsilon_{obsd}$ vs. K_{26} gives the value of ϵ_{HS} from the slope and that of ϵ_{LS} from the intercept. The temperature dependences of ϵ_{obsd} for aqueous solutions of [Fe(acac$_2$trien)]$^+$ and [Fe(Sal$_2$trien)]$^+$ at 520 and 503 nm, respectively, are given in Tables VI and VII (supplementary material). For [Fe(acac$_2$trien)]$^+$, values of 2503 ± 13 and 644 ± 8 M^{-1} cm^{-1} were obtained for ϵ_{HS} and ϵ_{LS}, respectively, at 520 nm, using eq 11. Similarly, for [Fe(Sal$_2$trien)]$^+$ values of 3506 ± 19 and 1575 ± 18 M^{-1} cm^{-1} were obtained for ϵ_{HS} and ϵ_{LS}, respectively, at 503 nm. Implicit in these calculations is the assumption that ϵ_{HS} and

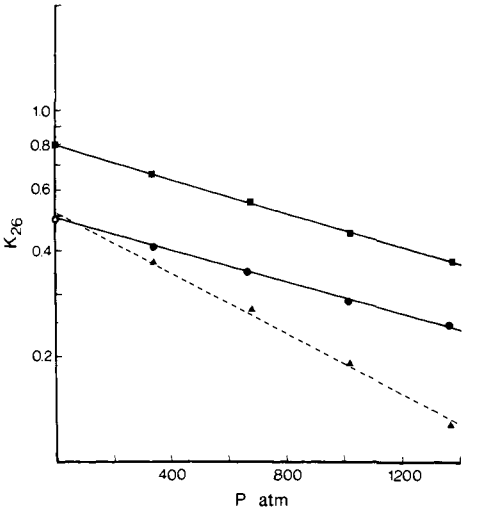

Figure 9. Plots of log K_{26} vs. P for [Fe(acac$_2$trien)]$^+$ (●) and [Fe(Sal$_2$trien)]$^+$ for $\mu_{LS} = 1.9\ \mu_B$ (■) and $\mu_{LS} = 3.0\ \mu_B$ (▲) in distilled water at 25 °C.

ϵ_{LS} are independent of temperature. If the further assumption is made that ϵ_{HS} and ϵ_{LS} are also independent of pressure, the pressure dependence of the equilibrium constants can be evaluated from the pressure dependence of the spectra by rearranging eq 11 to give the expression $K_{26} = (\epsilon_{LS} - \epsilon_{obsd})/(\epsilon_{obsd} - \epsilon_{HS})$.

The pressure dependences of the molar absorptivities, ϵ_{obsd}, for aqueous solutions of [Fe(acac$_2$trien)]$^+$ and [Fe(Sal$_2$trien)]$^+$ at 520 and 503 nm, respectively, are listed in Tables VIII and IX (supplementary material). The equilibrium constants calculated from these data are shown in Figure 9 as plots of log K_{26} vs. P. When such plots are linear, the value of $\Delta V°$ can be obtained from the slope by using the equation $\ln K_{26} = -(\Delta V°/RT)P$. For [Fe(acac$_2$trien)]$^+$ the plot appears linear, yielding a value of 12.7 ± 0.3 cm^3 mol^{-1} for $\Delta V°$, in quite good agreement with the value of 10.3 ± 0.2 cm^3 mol^{-1} obtained from the relaxation amplitudes. However, in the case of [Fe(Sal$_2$trien)]$^+$ the plot of log K_{26} vs. P is nonlinear, which may be due to a compressibility difference between the isomers, resulting in $\Delta V°$ being pressure dependent.[23]

(23) Lown, D. A.; Thirsk, H. R.; Lord Wynne-Jones *Trans. Faraday Soc.* **1968**, *64*, 2073.

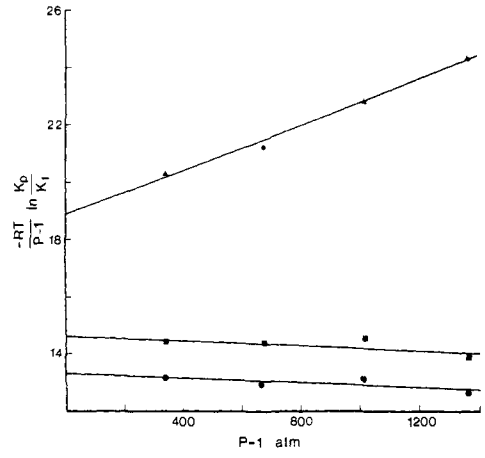

Figure 10. Plots of $[-RT/(P-1)]\ \ln (K_p/K_1)$ vs. $(P-1)$ for $[Fe(acac_2trien)]^+$ (●) and $[Fe(Sal_2trien)]^+$ for $\mu_{LS} = 1.9\ \mu_B$ (■) and $\mu_{LS} = 3.0\ \mu_B$ (▲) in distilled water at 25 °C.

The limiting value of ΔV° at 1 atm, ΔV_1°, can be determined in such cases by using eq 12, where $\Delta\kappa_1^\circ$ is the change in com-

$$\frac{-RT}{(P-1)} \ln\left(\frac{K_p}{K_1}\right) = \Delta V_1^\circ - 1/2\Delta\kappa_1^\circ(P-1) \qquad (12)$$

pressibility ($cm^3\ mol^{-1}\ atm^{-1}$) and K_p and K_1 are the equilibrium constants at P and 1 atm, respectively.[23] With use of this procedure, a value of 13.3 $cm^3\ mol^{-1}$ for ΔV_1° is calculated for $[Fe(acac_2trien)]^+$ (Figure 10), in good agreement with the value obtained from fitting the data as $\ln K_{26}$ vs. P and with the value obtained from the relaxation amplitudes. For $[Fe(Sal_2trien)]^+$, however, the ΔV_1° of 18.9 ± 0.3 $cm^3\ mol^{-1}$ obtained in this way is not in good agreement with the value of 11.9 ± 0.1 $cm^3\ mol^{-1}$ obtained from the relaxation amplitudes. However, the fitting procedure for the temperature and pressure dependence of the spectra is sensitive to the thermodynamic parameters for the spin equilibrium. Since Wilson et al. have found the magnetic moment to be anion dependent in solution,[7] ion association may affect the values of the thermodynamic parameters determined at relatively high concentrations by the NMR method. At the low concentrations used for the spectroscopic measurements, however, no significant ion association would be expected and the magnetic moments and thermodynamic parameters may well be different from those obtained by the NMR method. The apparent change in compressibility of $[Fe(Sal_2trien)]^+$ may be due solely to the use of inapplicable equilibrium constants in fitting the temperature and pressure dependence of the spectrum.

To illustrate this possibility, if limiting moments of 5.92 and 1.9 μ_B are used to calculate the equilibrium constants, then although the plot of $\log K_{26}$ vs. T^{-1} is curved, a respectable least-squares fit is obtained, yielding a ΔH° of 4.06 ± 0.06 kcal mol^{-1} and a ΔS° of 13.2 ± 0.2 cal $deg^{-1}\ mol^{-1}$. With these values a straight line plot is obtained for $\log K_{26}$ vs. P (Figure 9), yielding a ΔV° of 14.0 ± 0.2 $cm^3\ mol^{-1}$, while a value of 14.3 ± 0.3 $cm^3\ mol^{-1}$ is obtained for ΔV_1° (Figure 10). These volume differences are self-consistent and close to those obtained for $[Fe(acac_2trien)]^+$. Clearly, the latter values of ΔH° and ΔS° fit the temperature and pressure dependence of the spectrum for $[Fe(Sal_2trien)]^+$ in water quite well.[35] These values are also remarkably close to the thermodynamic parameters obtained in methanol solution. However, with use of a ΔH° of 4.06 kcal mol^{-1} and a ΔS° of 13.2 cal $deg^{-1}\ mol^{-1}$, the ultrasonic relaxation amplitudes give ΔV° values of 9.7, 10.8, and 11.0 $cm^3\ mol^{-1}$ at 5, 15, and 25 °C, respectively, the trend with temperature indicating unsatisfactory agreement between the relaxation amplitudes and these thermodynamic parameters. This suggests that the thermodynamic parameters are concentration dependent since the ultrasonic relaxation measurements are too precise to account for such a large trend of ΔV° values with temperature. Since the ultrasonic and NMR measurements were performed close to the solubility limit of $[Fe(Sal_2trien)]NO_3 \cdot H_2O$ in water, it appears likely that there are specific solvent–solute effects on these measurements. Under these conditions it is more appropriate to use a ΔH° of 5.11 kcal mol^{-1} and a ΔS° of 15.7 cal $deg^{-1}\ mol^{-1}$ in treating the ultrasonic relaxation data.

To investigate further the possible concentration dependence of spin equilibria, we followed the relaxations spectrophotometrically by using the laser temperature-jump technique at 510 nm for $[Fe(acac_2trien)]^+$ and at 503 nm for $[Fe(Sal_2trien)]^+$, which correspond to the peak maxima of the respective high-spin bands at room temperature (Figures 7 and 8). For $[Fe(acac_2trien)]NO_3$ measurements were made at 0.05 M in an aqueous 10^{-4} M KOH medium by using a 0.1-mm path length cell, the final temperature, T_∞, being 30 ± 2 °C. The spin state relaxation was observed to occur within the heating risetime of the apparatus,[24] implying a relaxation time less than ~13 ns. Similar results were obtained for 0.005 and 0.05 M solutions of the complex in methanol at T_∞ values of 25 ± 2 °C.

For $[Fe(Sal_2trien)]NO_3 \cdot H_2O$ measurements were made for 0.0025 and 0.025 M solutions in distilled water at T_∞ values of 25 ± 2 and 30 ± 2 °C, respectively, and for 0.002 and 0.02 M solutions in methanol at T_∞ values of 25 ± 2 °C. In all cases the spin state relaxations were observed to occur within the ~13-ns heating rise time. These results are consistent with our previous observation of a relaxation time of 5.33 ± 0.05 ns at 25 °C for $[Fe(Sal_2trien)]^+$ in distilled water, using the ultrasonic relaxation technique.[4] Similarly, rapid relaxations were also observed for aqueous and methanol solutions at T_∞ values of 10 ± 2 °C and 5 ± 2 °C, respectively.

Discussion

Solutions of $[Fe(acac_2trien)]NO_3$ in aqueous media exhibit single ultrasonic relaxation processes with concentration-independent relaxation times (for 0.02–0.10 M solutions), as expected for a unimolecular isomerization between two states of different spin multiplicity. The observed relaxation time of 2.11 ± 0.04 ns at 25 °C in pH 10 buffer is identical with our previously reported preliminary value of 2.12 ± 0.06 ns at 25 °C in distilled water[4] and is consistent with the results of our laser temperature-jump experiments, which imply that the relaxation time is less than ~13 ns. Similarly, we have previously reported observations of single ultrasonic relaxation processes for solutions of $[Fe(Sal_2trien)]NO_3 \cdot H_2O$ in distilled water, with the relaxation time of 5.33 ± 0.05 ns at 25 °C being concentration independent over the twofold concentration range (0.0127–0.0253 M) experimentally accessible.[4] This value is also consistent with our laser temperature-jump experiments which imply that the relaxation time at 25 °C is less than ~13 ns in distilled water. While Wilson et al. have reported a value of 38 ± 4 ns for the relaxation time at 4 °C in water using the laser temperature-jump technique,[6,7] our temperature-jump measurements at 10 °C revealed only the ~13-ns heating rise time, consistent with the value of 8.94 ± 0.16 ns at 5 °C obtained previously by using the ultrasonic relaxation technique.[4] Hence, for aqueous solutions of both $[Fe(acac_2trien)]^+$ and $[Fe(Sal_2trien)]^+$ our temperature-jump and ultrasonic measurements indicate rapid, apparently concentration-independent, relaxations of the spin equilibria. Since the amplitude of an ultrasonic relaxation depends both on concentration and the relaxation time (eq 9), the linear concentration dependences of the relaxation amplitudes for $[Fe(acac_2trien)]^+$ (Table I) and $[Fe(Sal_2trien)]^+$ (Table V) also indicate that the relaxation times are concentration independent. Finally, the temperature dependences of the relaxation amplitudes are consistent with those of the spin equilibria. The ultrasonic relaxations are therefore ascribed to unimolecular isomerizations of the iron(III) complexes between two states of different spin multiplicity.

(24) The heating risetime of the apparatus was tested using a 0.3 M solution of $K_4Fe(CN)_6$ in H_2O at 25 °C, for which the ion-association relaxation time is less than 1 ns. Under these conditions the observed $1/e$ time of ~13 ns is the heating rise time.

Previous measurements by Wilson et al. have suggested concentration dependent lifetimes for [Fe(acac$_2$trien)]PF$_6$ and [Fe(Sal$_2$trien)]PF$_6$ in methanol.[6,7,19] For concentrations above 10^{-3} M,[26] relaxation times $\leq$30 ns[25] are reported in ref 6, in agreement with our observations. However, for concentrations in the $\sim 10^{-4}$ M range,[26] relaxation times significantly longer than the heating rise time are reported in ref 7 and 19. Under the conditions of the latter experiments the sample absorbance at the detection wavelength was less than 0.1.[19,28] Judging from the temperature dependence of the spectra, the relaxation amplitude would have been close to the limits of detectability[19,28] and hence unreliable. On the basis of our ultrasonic and laser temperature-jump results, it therefore seems more reasonable to consider the spin state relaxations as independent of concentration.

The volume differences, $\Delta V°$, between the high-spin and low-spin states of both [Fe(acac$_2$trien)]$^+$ and [Fe(Sal$_2$trien)]$^+$, as evaluated from the ultrasonic relaxation amplitudes, are constant with temperature and are similar, as expected for these structurally related complexes. These $\Delta V°$ values may be used to estimate the changes in metal–ligand bond lengths accompanying the spin state isomerizations, using eq 13, if either r_{HS} or r_{LS}, the effective

$$\Delta V° = N_A \frac{4\pi}{3}(r_{HS}^3 - r_{LS}^3) \qquad (13)$$

packing radii of the two spin states, is known. To estimate the packing radii in solution, one must know how closely on average the solvent molecules approach the complexes. In the solid state the molecular packings of [Fe(Sal$_2$trien)]Cl·2H$_2$O and [Fe(Sal$_2$trien)]NO$_3$·H$_2$O consist of cations linked by hydrogen bonding to water and anions as (–cation–water–anion–cation–) infinite chains.[20] The sites of hydrogen bonding to the cation are the amine hydrogen atoms, showing that there is relatively free access to the donor atoms. The strong hydrogen bonding in the solid state has been shown to persist in solution from the solvent dependence of the N–H stretching frequency in the infrared spectrum.[7] The free access of solvent molecules to the donor atoms at hydrogen bonding and van der Waals' contacts implies that much of the ligand is solvated. Therefore, while the bulk of the ligand contributes to the total molar volume, those parts which are fully solvated will not contribute to the change in volume upon an expansion of the coordination sphere, i.e., they will occupy the same volume in both spin states. Hence, the large, average spherical radii, which can be obtained from the partial molal volumes of the complexes in solution,[27] cannot be used with the $\Delta V°$ values to calculate realistic metal–ligand bond length differences between spin states by using eq 13. From the X-ray crystal structure data for these complexes[20] it appears that a most reasonable value for the low-spin packing radius, r_{LS}, of both [Fe(acac$_2$trien)]$^+$ and [Fe(Sal$_2$trien)]$^+$ is the average low-spin metal–ligand bond length of 1.94 Å[20] plus the average van der Waals radius of the donor atoms of 1.47 Å. With use of this value of 3.41 Å for the low-spin packing radius in solution, the $\Delta V°$ values of 10.3 and 11.9 cm^3 mol^{-1} correspond to differences in average metal–ligand bond lengths of 0.11 and 0.13 Å between the doublet and sextet spin states of [Fe(acac$_2$trien)]$^+$ and [Fe(Sal$_2$trien)]$^+$, respectively. These values are in excellent agreement with the average metal–ligand bond length difference of 0.126 Å between low-spin (1.94 μ_B) [Fe(Sal$_2$trien)]Cl·2H$_2$O and high-spin (5.99 μ_B) [Fe(acac$_2$trien)]PF$_6$.[20] This further confirms the assignments of the ultrasonic relaxations to unimolecular isomerization processes between the doublet and sextet states of both [Fe(acac$_2$trien)]$^+$ and [Fe(Sal$_2$trien)]$^+$.

(25) See footnote 51 in ref 19.
(26) Wilson, L. J., personal communication, Rice University, Houston, Texas 77001.
(27) Binstead, Robert A. Ph.D. Thesis, The University of Sydney, 1979.
(28) (a) The molar absorptivities at the observation wavelengths used by Wilson et al. are 1800 M^{-1} cm^{-1} for [Fe(acac$_2$trien)]$^+$ and 2750 M^{-1} cm^{-1} for [Fe(Sal$_2$trien)]$^+$. The cell path length used was 0.081 cm. (b) The visible spectrum of [Fe(Sal$_2$trien)]NO$_3$·H$_2$O in methanol was determined at 15, 25 and 35 °C. The molar absorptivities at 495 nm, corrected for changes in concentration with temperature, were 2580, 2750, and 2900 M^{-1} cm^{-1}, respectively.

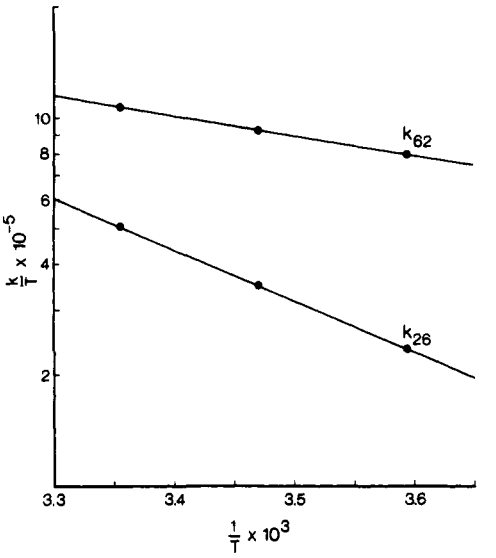

Figure 11. Eyring plots of the temperature dependence of the rate constants k_{26} and k_{62} for [Fe(acac$_2$trien)]NO$_3$ in pH 10 buffer.

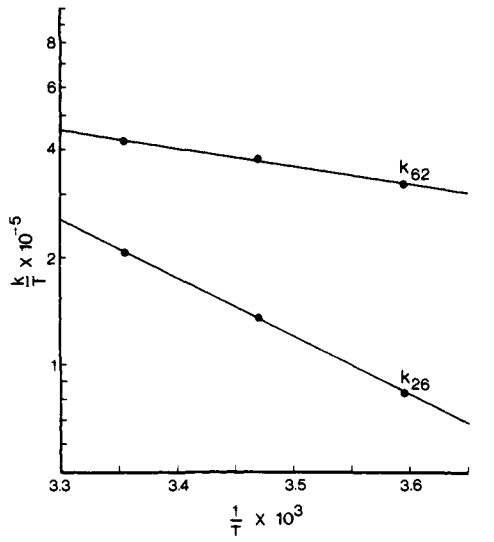

Figure 12. Eyring plots of the temperature dependence of the rate constants k_{26} and k_{62} for [Fe(Sal$_2$trien)]NO$_3$·H$_2$O in H$_2$O.

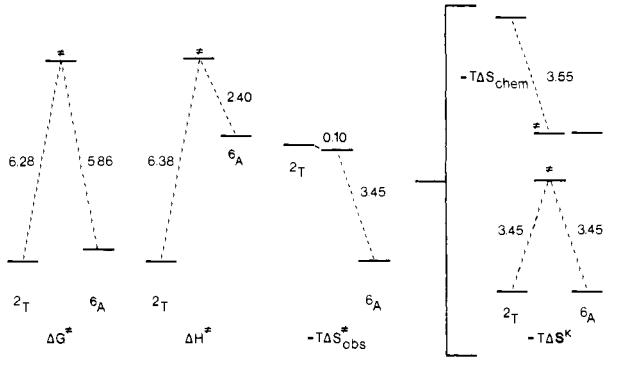

Figure 13. Activation parameters for [Fe(acac$_2$trien)]NO$_3$ in pH 10 buffer with $-T\Delta S_{obsd}^{\neq}$ partitioned to give the minimum value of κ.

The rate constants for the intersystem crossing between spin states can be calculated from the relaxation times. For a unimolecular isomerization process between the low-spin doublet and high-spin sextet states:

$$\tau^{-1} = k_{26} + k_{62} = k_{62}(K_{26} + 1) \qquad (14)$$

With use of the equilibrium constants determined by the NMR method, the rate constants given in Tables I and V are calculated.

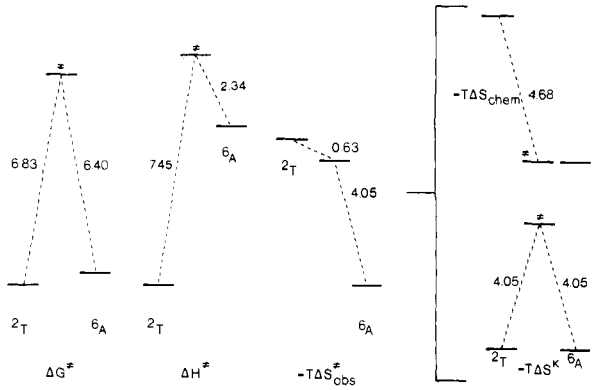

Figure 14. Activation parameters for $[Fe(Sal_2trien)]NO_3 \cdot H_2O$ in H_2O with $-T\Delta S_{obsd}^{\ddagger}$ partitioned to give the minimum value of κ.

The most significant aspect of these results is the temperature dependence of the rate constants (Figures 11 and 12). The free-energy barriers calculated from the rate constants at 25 °C and the activation parameters obtained from their temperature dependence using absolute rate theory (eq 15) are listed in Tables

$$k = \left(\frac{k_B T}{h}\right) e^{-\Delta G_{obsd}^{\ddagger}/RT} = \left(\frac{k_B T}{h}\right) e^{-\Delta H_{obsd}^{\ddagger}/RT} e^{\Delta S_{obsd}^{\ddagger}/R} = \kappa \left(\frac{k_B T}{h}\right) e^{-\Delta H_{obsd}^{\ddagger}/RT} e^{\Delta S^{\ddagger}/R} \quad (15)$$

I and V and illustrated in Figures 13 and 14. An assessment of the magnitude of κ, the transmission coefficient, which reflects the probability of the spin-forbidden intersystem crossing, can be made from these results in the manner described previously.[4]

A minimum value of κ and hence the lowest probability of intersystem crossing is obtained by assuming that the entropy of the transition state equals that of the high-spin sextet state. If the entire entropic barrier of 3.45 kcal mol^{-1} is due to κ, the minimum value of κ is $10^{-2.5}$. For $[Fe(Sal_2trien)]^+$ a similar analysis of the activation parameters leads to a smaller estimate of $10^{-3.0}$ for κ.[36] This may be compared with the minimum value of $10^{-3.4}$ reported for κ in our previous work,[4] in which the equilibrium constants and thermodynamic parameters were based on a value of 1.9 μ_B for μ_{LS} instead of 3.0 μ_B as determined by the more accurate measurements in this work. Thus, the determination of κ is not very sensitive to small errors in the equilibrium constants.

Examination of the X-ray crystal structures of $[Fe(acac_2trien)]^+$ and $[Fe(Sal_2trien)]^+$ reveals distortions from octahedral symmetry which would be expected to split the ^2T states into ^2A and ^2E states. The effect of the splitting is to introduce a degeneracy barrier into the intersystem-crossing processes and hence increase the minimum probability of intersystem crossing, κ, to $10^{-2.4}$ (^2E) or $10^{-2.1}$ (^2A) for $[Fe(acac_2trien)]^+$ and to $10^{-2.8}$ (^2E) or $10^{-2.5}$ (^2A) for $[Fe(Sal_2trien)]^+$.

For both $[Fe(acac_2trien)]^+$ and $[Fe(Sal_2trien)]^+$ the activation free energies $\Delta G_{26}^{\ddagger}$ of 6.28 and 6.82 kcal mol^{-1}, respectively, are almost entirely due to the activation enthalpies $\Delta H_{26}^{\ddagger}$ of 6.38 and 7.45 kcal mol^{-1}, respectively. Within experimental error there is in fact no significant difference between the activation free energies and activation enthalpies. This implies a correlation between the magnitude of the transmission coefficient, κ, and the chemical entropy of the activated complex. If $\kappa \approx 1$, the entropy of the transition state is that of the low-spin doublet state; if κ approaches its minimum value, the entropy of the activated complex approaches that of the high-spin sextet state. Although a strong inference cannot be drawn, it is likely that the entropy of the activated complex is closer to that of the high-spin state than of the low-spin state, implying that κ is closer to $10^{-2.5}$ and $10^{-3.0}$ than to 1 for $[Fe(acac_2trien)]^+$ and $[Fe(Sal_2trien)]^+$, respectively. This is suggested by the observation that the overall free-energy changes for these spin state transitions are close to zero, so that the enthalpic differences are compensated by the entropic differences. Since the enthalpies of the transition states are closer to those of the high-spin states, their entropies may similarly resemble those of the high-spin states.

This interpretation is physically reasonable if the higher enthalpy of the activated complex is due to an expansion of the coordination sphere to resemble the larger high-spin state. Such an activated complex would possess greater entropy owing to increased vibrational partition functions, a consequence of longer, weaker metal–ligand bonds, and decreased solvation. The determination of the volumes of activation experimentally, however, requires the more difficult measurements of relaxation times as a function of applied pressure. In the absence of such data it can only be surmised that $\Delta V_{26}^{\ddagger} \approx \Delta V_{26}^{\circ}$, i.e., the transition state resembles the high-spin sextet state, and that κ is therefore of the order of 10^{-2}–10^{-3} for these iron(III) $\Delta S = 2$ intersystem-crossing processes.

From the results obtained previously for $[Fe(paptH)_2]^{2+}$ the minimum value of κ was found to be $10^{-2.5}$, again assuming the absence of a minimum in $-T\Delta S^{\ddagger}$ between the two spin states.[3] This implies that for *these* iron(II) and iron(III) complexes there is no significant difference in the probability of the $\Delta S = 2$ intersystem-crossing process and that for these systems κ lies within an order of magnitude of 10^{-2}.

With use of the Landau–Zener model, the transmission coefficient, κ, can be interpreted in terms of the interaction energy between two potential energy surfaces at the crossing point.[29] With the assumption that both surfaces can be represented by identical harmonic oscillators with a fundamental frequency of 300 cm^{-1} and reduced mass of 50, separated by 0.1 Å, a transmission coefficient $\kappa \approx 10^{-2}$ implies an energy separation of ~38 cm^{-1}. This result may be compared with the theoretical treatments of König and Kremer for d^5 and d^6 spin equilibria.[30-34] Although these treatments are mainly concerned with the calculations of the temperature dependences of the magnetic moments of d^5 and d^6 spin equilibria, the full calculations of the behavior of the energy levels close to the crossover points reveal that there are significant interactions between the ground states at or near the formal crossover points. These interactions result from spin-orbit coupling of the ground states with the low-lying ^4T (d^5 systems) and ^3T (d^6 systems) excited states, providing a mechanism for intersystem crossing.

For d^5 systems this interaction occurs between the Γ_7 (^6A) and Γ_7 (^2T) spin–orbit levels.[31] Since these are the lowest lying levels of each spin state, the mechanistic and formal crossover points are coincident. For d^6 systems the formal crossover point is defined as the intersection of the Γ_1 (^1A) and Γ_5 (^5T) spin–orbit levels.[32,33] However, these levels do not interact either on the basis of spin–orbit coupling or configuration interaction, i.e., these levels remain very pure at the formal crossover point.[33] This would suggest a much smaller value of κ for d^6 than for d^5 configurations. However, König and Kremer have shown that there is significant interaction between the Γ_1 (^1A) and Γ_1 (^5T) levels ~400 cm^{-1} above the ground level and at a $10Dq$ value ~200 cm^{-1} below the formal crossover point.[32,33] Since the ^1A and ^5T states can only mix via spin–orbit levels with the same irreducible representation the mechanistic crossover between the ^1A and ^5T states occurs between the ^1A state and one of the higher energy spin–orbit levels of the ^5T manifold at ~200 cm^{-1} below the formal crossover

(29) Kauzman, W. "Quantum Chemistry"; Academic Press: New York, 1957; p 541.
(30) König, E.; Kremer, S. *Ber. Bunsenges. Phys. Chem.* **1974**, *78*, 268.
(31) König, E.; Schnakig, R.; Kremer, S. *Z. Naturforsch., A* **1974**, *29A*, 419.
(32) König, E.; Kremer, S. *Theor. Chim Acta* **1971**, *22*, 45.
(33) König, E.; Kremer, S. *Theor. Chim. Acta* **1972**, *26*, 311.
(34) König, E.; Kremer, S. *Ber. Bunsenges. Phys. Chem.* **1972**, *76*, 870.
(35) For $[Fe(Sal_2trien)]^+$ values of 3519 ± 11 and 1159 ± 15 M^{-1} cm^{-1} are obtained for ϵ_{HS} and ϵ_{LS}, respectively, at 503 nm by assuming a ΔH° of 4.06 kcal mol^{-1} and a ΔS° of 13.2 cal deg^{-1} mol^{-1}.
(36) When a value of 1.90 μ_B for μ_{LS} is assumed, the activation parameters are calculated to be $\Delta H_{26}^{\ddagger} = 6.17 \pm 0.26$ kcal mol^{-1}, $\Delta S_{26}^{\ddagger} = -1.6 \pm 0.9$ cal deg^{-1} mol^{-1}, $\Delta H_{62}^{\ddagger} = 2.11 \pm 0.26$ kcal mol^{-1} and $\Delta S_{62}^{\ddagger} = -14.8 \pm 0.9$ cal deg^{-1} mol^{-1}. These values lead to a lower limit for κ of $10^{-3.2}$, compared with a value of $10^{-3.0}$ obtained by using a value of 3.0 μ_B for μ_{LS}.

point and ~400 cm^{-1} above the ground level of the ^5T manifold.

The magnitude of the interaction energy is ~100 cm^{-1} for both d^5 and d^6 systems,[31-33] implying that intersystem crossing is not highly forbidden for either d^5 or d^6 spin equilibria. This is certainly consistent with the lower limits for κ of 10^{-2}-10^{-3} obtained for $[Fe(acac_2trien)]^+$, $[Fe(Sal_2trien)]^+$, and $Fe(paptH)_2]^{2+}$. However, the smaller minimum value for κ of $10^{-4.2}$ found for $[Fe(HB(pz)_3)_2]$ may indicate differences in the extent of mixing at the crossover point among different complexes.[3]

In summary, ultrasonic absorption measurements for aqueous solutions of $[Fe(acac_2trien)]^+$ reveal single ultrasonic relaxation processes with the relaxation time of 2.11 ± 0.04 ns at 25 °C being concentration independent over the range 0.02-0.10 M. This is similar to the results obtained previously for $[Fe(Sal_2trien)]^+$, for which a relaxation time of 5.33 ± 0.05 ns was observed at 25 °C in distilled water.[4] These values for the relaxation times are consistent with the results of our laser temperature-jump experiments for aqueous and methanol solutions of the complexes, which also reveal no apparent concentration dependence of the relaxation times. Independent estimates for the volume differences, $\Delta V°$, obtained from the pressure dependence of the spectra are consistent with the values obtained from the ultrasonic relaxation amplitudes. The temperature dependences of the ultrasonic relaxation amplitudes are also consistent with the temperature dependences of the spin equilibria as determined from magnetic susceptibility measurements. The ultrasonic relaxations are therefore ascribed to unimolecular isomerizations of the iron(III) complexes between two states of different spin multiplicity. With use of the $\Delta V°$ values obtained from the ultrasonic relaxation amplitudes, the average metal-ligand bond length differences between the two spin states are calculated to be 0.11 and 0.13 Å for $[Fe(acac_2trien)]^+$ and $[Fe(Sal_2trien)]^+$, respectively, in excellent agreement with the X-ray structural data for these complexes.[20]

The accuracy of the ultrasonic relaxation technique permits the evaluation of the activation parameters for these formally spin-forbidden $\Delta S = 2$ intersystem-crossing processes, revealing significant activation enthalpies in *both* directions. With use of absolute rate theory, the minimum value of the transmission coefficient is $10^{-2.5}$ for $[Fe(acac_2trien)]^+$ and $10^{-3.0}$ for $[Fe(Sal_2trien)]^+$. Thus, both thermodynamic barriers and electronic factors contribute substantially to the free-energy barriers for intersystem crossing in these iron(III) complexes. Therefore, the intersystem-crossing process in these systems can be described as a nonadiabatic, internal electron transfer between two distinct electronic isomers possessing different nuclear configurations, with the average metal-ligand bond length difference being 0.11-0.13 Å. Finally, it should be noted that unimolecular excited-state decay processes can compete with intersystem-crossing processes, so that κ values of ~10^{-2} will be important in determining the observed quantum yields of such processes.

Acknowledgment. The work at the University of Sydney was sponsored in part by the Australian Research Grants Committee and in part by the Sydney County Council. Acknowledgement if also made to the donors of The Petroleum Research Fund, administered by the American Chemical Society, for partial support of this work. The work at the University of Rochester was sponsored by NIH under Grants GM 22939-04 and 5T32GM07230. D.H.T. is an Alfred P. Sloan Fellow. We thank Dr. G. A. Lawrance for assistance with the high-pressure measurements at the University of Melbourne.

Supplementary Material Available: Tables II, III, and IV of the solution magnetic susceptibility data and Tables VI, VII, VIII, and IX of variable temperature/pressure spectral data (7 pages). Ordering information is given on any current masthead page.

Dynamic Properties of Phosphinehydridorhodium(I) Complexes and the Structure of Tris(triisopropylphosphine)hydridorhodium(I), $RhH(P(i\text{-}Pr)_3)_3$

T. Yoshida,[1a] David L. Thorn,[1b] T. Okano,[1a] Sei Otsuka,[1a] and James A. Ibers*[1b]

Contribution from the Department of Chemistry, Faculty of Engineering Science, Osaka University, Toyonaka, Osaka, Japan 560, and the Department of Chemistry, Northwestern University, Evanston, Illinois 60201. *Received March 12, 1980*

Abstract: The phosphinehydridorhodium(I) complexes $RhH(P(i\text{-}Pr)_3)_3$ (1) and $RhH(PEt_3)_3$ (2) undergo an intramolecular site exchange process similar to that of $RhH(PPh_3)_3$. In an attempt to understand this process, the crystal and molecular structure of tris(triisopropylphosphine)hydridorhodium(I), $RhH(P(i\text{-}Pr)_3)_3$ (1), has been determined at -150 °C. The complex crystallizes as yellow needles with two formula units in the triclinic space group C_i^1-$P\bar{1}$ in a cell of dimensions a = 11.615 (5) Å, b = 16.958 (8) Å, c = 8.680 (6) Å, α = 103.44 (2)°, β = 103.53 (2)°, γ = 82.98 (2)°, V = 1612 Å^3. The final conventional and weighted agreement indices on F_o for 7082 reflections with $F_o^2 > 3\sigma(F_o^2)$ are 0.025 and 0.029, respectively. The molecule exhibits strictly planar coordination about the rhodium atom but the steric bulk of the triisopropylphosphine ligands has caused some unusual angular distortions about the rhodium and phosphorus atoms. The H-Rh-P(cis) angle is 70.7 (14)° (av), the smallest reported for planar structures. The Rh-P-C angles, usually in the range 111-117° in rhodium triisopropylphosphine complexes, span the range 109.28 (6) to 126.38 (6)° in the present complex. The Rh-H distance is 1.58 (2) Å, Rh-P (trans to H) is 2.330 (1) Å, and Rh-P (cis to H) are 2.291 (1) and 2.297 (1) Å. The difference in stereochemical rigidity of $RhH(PR_3)_3$ may be ascribed primarily to the steric requirements of the phosphine ligands. The tetrakisphosphine complex $RhH(PEt_3)_4$ (3) exists in equilibrium with 2 and PEt_3 and also is fluxional.

Introduction

We have recently studied the unusual coordination numbers and geometries imposed upon rhodium complexes by bulky phosphine ligands.[2-7] In earlier papers we have discussed the formation and properties of hydridodinitrogen rhodium bis(trialkyl)phosphine complexes,[2,5] and their tendency to lose the di-

(1) (a) Osaka University; (b) Northwestern University.

(2) Hoffman, P. R.; Yoshida, T.; Okano, T.; Otsuka, S.; Ibers, J. A. *Inorg. Chem.*, **1976**, *15*, 2462-2466.

(3) Yoshida, T.; Okano, T.; Otsuka, S. *J. Chem. Soc., Chem. Commun.*, **1978**, 855-856.

0002-7863/80/1502-6451$01.00/0